The American Journal of Pathology, Vol. 185, No. 2, February 2015

ELSEVIER

The American Journal of PATHOLOGY

ajp.amjpathol.org

IMMUNOPATHOLOGY AND INFECTIOUS DISEASES

Type I Interferon Contributes to Noncanonical Inflammasome Activation, Mediates Immunopathology, and Impairs Protective Immunity during Fatal Infection with Lipopolysaccharide-Negative Ehrlichiae

Qin Yang,* Heather L. Stevenson,* Melanie J. Scott,† and Nahed Ismail*

From the Departments of Pathology and Surgery,† School of Medicine, University of Pittsburgh, Pittsburgh, Pennsylvania*

Accepted for publication October 9, 2014.

Address correspondence to Nahed Ismail, M.D., Ph.D., Department of Pathology, University of Pittsburgh, S739-Scaife Hall, 3550 Terrace St., Pittsburgh, PA 15261. E-mail: ismailn@upmc.edu.

Ehrlichia species are intracellular bacteria that cause fatal ehrlichiosis, mimicking toxic shock syndrome in humans and mice. Virulent ehrlichiae induce inflammasome activation leading to caspase-1 cleavage and IL-18 secretion, which contribute to development of fatal ehrlichiosis. We show that fatal infection triggers expression of inflammasome components, activates caspase-1 and caspase-11, and induces host-cell death and secretion of IL-1β, IL-1α, and type I interferon (IFN-I). Wild-type and *Casp1*$^{-/-}$ mice were highly susceptible to fatal ehrlichiosis, had overwhelming infection, and developed extensive tissue injury. *Nlrp3*$^{-/-}$ mice effectively cleared ehrlichiae, but displayed acute mortality and developed liver injury similar to wild-type mice. By contrast, *Ifnar1*$^{-/-}$ mice were highly resistant to fatal disease and had lower bacterial burden, attenuated pathology, and prolonged survival. *Ifnar1*$^{-/-}$ mice also had improved protective immune responses mediated by IFN-γ and CD4^{+} Th1 and natural killer T cells, with lower IL-10 secretion by T cells. Importantly, heightened resistance of *Ifnar1*$^{-/-}$ mice correlated with improved autophagosome processing, and attenuated noncanonical inflammasome activation indicated by decreased activation of caspase-11 and decreased IL-1β, compared with other groups. Our findings demonstrate that IFN-I signaling promotes host susceptibility to fatal ehrlichiosis, because it mediates ehrlichia-induced immunopathology and supports bacterial replication, perhaps via activation of noncanonical inflammasomes, reduced autophagy, and suppression of protective CD4^{+} T cells and natural killer T-cell responses against ehrlichiae. *(Am J Pathol 2015, 185: 446–461; http://dx.doi.org/10.1016/j.ajpath.2014.10.005)*

Ehrlichia chaffeensis is the causative agent of human monocytotropic ehrlichiosis, a highly prevalent life-threatening tickborne disease in North America.[1–3] Central to the pathogenesis of human monocytotropic ehrlichiosis is the ability of ehrlichiae to survive and replicate inside the phagosomal compartment of host macrophages and to secrete proteins via type I and type IV secretion systems into the host-cell cytosol.[4] Using murine models of ehrlichiosis, we and others have demonstrated that fatal ehrlichial infection is associated with severe tissue damage caused by TNF-α–producing cytotoxic CD8^{+} T cells (ie, immunopathology) and the suppression of protective CD4^{+} Th1 immune responses.[5–14] However, neither how the *Ehrlichia* bacteria trigger innate immune responses nor how these responses influence the acquired immunity against ehrlichiae is entirely known.

Extracellular and intracellular pattern recognition receptors recognize microbial infections.[15–18] Recently, members of the cytosolic nucleotide-binding domain and leucine-rich repeat family (NLRs; alias NOD-like receptors), such as NLRP3, have emerged as critical pattern recognition receptors in the host defense against intracellular pathogens. NLRs recognize intracellular bacteria and trigger innate, protective immune responses.[19–23] NLRs respond to both

Supported by NIH grants R56-AI097679-01A (N.I.) and R01-GM102146 (M.J.S.).

Disclosures: None declared.

http://dx.doi.org/10.1016/j.ajpath.2014.10.005

microbial products and endogenous host danger signals to form multimeric protein platforms known as inflammasomes. The NLRP3 inflammasome consists of multimers of NLRP3 that bind to the adaptor molecules and apoptosis-associated speck-like protein (ASC) to recruit pro−caspase-1 and facilitate cleavage and activation of caspase-1.[15,16,24] The canonical inflammasome pathway involves the cleavage of immature forms of IL-1β and IL-18 (pro−IL-1β and pro−IL-18) into biologically active mature IL-1β and IL-18 by active caspase-1.[25−28] The noncanonical inflammasome pathway marked by the activation of caspase-11 has been described recently. Active caspase-11 promotes the caspase-1−dependent secretion of IL-1β/IL-18 and mediates inflammatory lytic host-cell death via pyroptosis, a process associated with the secretion of IL-1α and HMGB1.[17,29−31] Several key regulatory checkpoints ensure the proper regulation of inflammasome activation.[16,32] For example, blocking autophagy by the genetic deletion of the autophagy regulatory protein ATG16L1 increases the sensitivity of macrophages to the inflammasome activation induced by TLRs.[33] Furthermore, TIR domain-containing adaptor molecule 1 (TICAM-1; alias TRIF) has been linked to inflammasome activation via the secretion of type I interferons α and β (IFN-α and IFN-β) and the activation of caspase-11 during infections with Gram-negative bacteria.[2,34−39]

We have recently demonstrated that fatal ehrlichial infection induces excess IL-1β and IL-18 production, compared with mild infection,[8,12−14] and that lack of IL-18 signaling enhances resistance of mice to fatal ehrlichiosis.[12] These findings suggest that inflammasomes play a detrimental role in the host defense against ehrlichial infection. Elevated production of IL-1β and IL-18 in fatal ehrlichiosis was associated with an increase in hepatic expression of IFN-α.[14] IFN-I plays a critical role in the host defense against viral and specific bacterial infections.[28,36,37,40−43] However, the mechanism by which type I IFN contributes to fatal ehrlichial infection remains unknown. Our present results reveal, for the first time, that IFNAR1 promotes detrimental inflammasome activation, mediates immunopathology, and impairs protective immunity against ehrlichiae via mechanisms that involve caspase-11 activation, blocking of autophagy, and production of IL-10. Our novel finding that lipopolysaccharide (LPS)-negative ehrlichiae trigger IFNAR1-dependent caspase-11 activation challenges the current paradigm that implicates LPS as the major microbial ligand triggering the noncanonical inflammasome pathway during Gram-negative bacterial infection.

Materials and Methods

Mice and Ehrlichial Infection *in Vivo*

The following mice, aged 8 to 12 weeks, were used: wild-type (WT) C57BL/6 (B6) (Jackson Laboratory, Bar Harbor, ME); *Nlrp3*$^{-/-}$ (NLR family, pyrin domain containing 3) (Millennium Pharmaceuticals, Boston, MA); *Casp1*$^{-/-}$ (a gift from Richard Flavell, Yale University, New Haven, CT)[44]; and *Ifnar1*$^{-/-}$ (B6.129S2-*Ifnar1*^{tm1Agt}/Mmjax; Mutant Mouse Regional Resource Center−Jackson Laboratory). All animals were housed under specific pathogen−free conditions at the University of Pittsburgh in accordance with institutional guidelines for animal welfare.

The highly virulent monocytotropic *Ixodes ovatus ehrlichia* (IOE) strain, provided by Dr. Yasuko Rikihisa (Ohio State University, Columbus, OH) was used. The IOE stock was propagated by passage through WT C57BL/6 mice. Single-cell suspensions from spleen of IOE-infected mice were collected on day 7 after infection (day 7 p.i.) and stored in liquid nitrogen for use as stocks. The mice were infected intraperitoneally with 1 mL of splenocytes containing approximately 10^3 IOE bacterial genomes per mouse. Mice were monitored daily for signs of illness and survival. At specified time points, three to five mice per experimental group were sacrificed, and the selected organs were harvested for further analysis.

Histology

Formalin-fixed, paraffin-embedded samples from the right lobe of the liver were collected on day 7 p.i. from each mouse group (before perfusion with phosphate-buffered saline) and then were sectioned and stained with hematoxylin and eosin. Histological sections were evaluated qualitatively for morphological differences and quantitatively for apoptosis (by TUNEL immunohistochemical assays). TUNEL staining (Research Histology Services, University of Pittsburgh) was performed on the formalin-fixed, paraffin-embedded tissue sections. Apoptotic Kupffer cells and hepatocytes were counted in 10 high-power fields for each mouse. Stained slides were viewed under an Olympus (Tokyo, Japan) BX40 microscope and were scanned using a Mirax MIDI slide scanner (Carl Zeiss Microscopy, Jena, Germany); images were captured using Pannoramic Viewer software (3DHistech, Budapest, Hungary).

Isolation of Liver Mononuclear Cells

Primary hepatocytes were isolated from the liver of mice according to the magnetic-activated cell sorting protocol (MACS; Miltenyi Biotec, Auburn, CA) for preparation of single-cell suspensions from mouse liver. In brief, the mouse liver was perfused *in situ* with cold phosphate-buffered saline via the portal vein. The liver tissue was homogenized using the Miltenyi Biotec gentleMACS program for liver, and the samples were incubated at room temperature for 45 minutes under slow continuous rotation. The resulting homogenate was passed through a 100-μm cell strainer (BD Biosciences, San Jose, CA) and centrifuged at 20 × *g* for 4 minutes to remove contaminating hepatocytes. After washing of cells and lysis of red blood cells, the cells were resuspended in complete medium (RPMI 1640 medium supplemented with 10% heat-inactivated fetal bovine serum, 1% HEPES buffer, and 100 μg/mL penicillin and streptomycin) (Gibco; Life

Technologies, Carlsbad, CA) and counted by trypan blue exclusion to examine viability before use for flow cytometry.

Flow Cytometry and Intracellular Cytokine Staining

Liver mononuclear cells and splenocytes were resuspended in staining buffer for fluorescence-activated cell sorting at a concentration of 10^6 cells per well. FcRs were blocked with a monoclonal antibody (clone 2.4G2) against mouse cell surface antigens CD16 and CD32 for 15 minutes. Antibodies were conjugated with fluorescein isothiocyanate, phycoerythrin, PerCP−Cy5.5, Alexa Fluor 488 dye, or allophycocyanin. The following antibodies were purchased from either BD Biosciences or BioLegend (San Diego, CA; antibodies were used at the concentrations recommended by the manufacturer): anti-CD3 (clone 145-2C11), anti-CD11c (clone HL3), anti-CD4 (clone RM4-4), anti-CD8a (clone 53-6.7), anti-CD25 (clone PC61), anti-CD11b (clone M1/70), anti-NK1.1 (clone PK136), anti-B220 (clone RA3-6B2), anti−IL-10 (clone JES5-16E3), anti−IFN-γ (clone XMG102), anti-Ly6G (clone 1A8), anti−granzyme B (clone NGZB). Anti−α-GalCer−loaded CD1d tetramer was a gift from Dr. Luc Van Kaer (Vanderbilt University, Nashville, TN). Isotype control monoclonal antibodies were fluorescein isothiocyanate−, phycoerythrin−, or allophycocyanin-conjugated hamster IgG1 (A19-3), rat IgG1 (R3-34), rat IgG2α (R35-95), mouse IgG2α (X39), mouse IgG2b (MPC-11), mouse IgG1 (X40), and rat IgG2b (A95-1). For intracellular cytokine staining, the splenocytes were incubated with BD GolgiPlug (BD Biosciences). Lymphocyte and granulocyte populations were gated based on forward and side-scatter parameters. Approximately 50,000 events for spleen cells and 100,000 events for liver mononuclear cells were collected using BD-LSR and BD FACSCalibur (Immunocytometry Systems; BD Biosciences) flow cytometry. Data were analyzed using FlowJo software version 7.5.5 (TreeStar, Ashland, OR).

Measurement of Cytokine Levels by Enzyme-Linked Immunosorbent Assay

Spleens were harvested and single-cell suspensions were prepared as described previously.[5–8] Splenocytes (2×10^6 to 5×10^6) were seeded into 12-well culture plates in complete medium in the presence or absence of IOE antigens. Culture supernatants were collected after 24 or 48 hours. Concentration of IL-1β, IL-10, and IFN-γ in supernatant and serum was determined using a murine enzyme-linked immunosorbent assay kit (eBioscience, San Diego, CA; Vienna, Austria) according to the manufacturer's recommendations. The minimum detectable concentrations of IL-1β, IL-10, and IFN-γ were 1.2 pg/mL, 5 pg/mL, and 5.3 pg/mL, respectively.

Analysis of Bacterial Burden by Quantitative Real-Time PCR

Relative differences in bacterial burden were measured by quantitative real-time PCR using an iCycler IQ multicolor real-time detection system (Bio-Rad Laboratories, Hercules, CA) and primers and probes for the ehrlichia *dsb* gene and *Gapdh*, as described previously.[6,9] The ehrlichia primer and probe sets used were EM/IOE dsb forward, 5′-CAGGATGGTAAAGTACGTGTGA-3′; EM/IOE dsb reverse, 5′-TAGCTAAYGCTGCCTGGACA-3′; EM/IOE probe: (6FAM)-AGGGATTTCCCTATACTCGGTGAGGC-(MGB-BHQ). The eukaryotic housekeeping gene *Gapdh* was amplified using the following primer and probe set: GAPDH forward, 5′-CAACTACATGGTCTACATGTTC-3′; GAPDH reverse, 5′-TCGCTCCTGGAAGATG-3′; GAPDH probe: (6FAM)-CGGCACAGTCAAGGCCGAGAATGGGAAGC-(MGB-BHQ). Results were normalized to the levels of the *Gapdh* gene in the same samples. The comparative cycle threshold (C_T) method was used to determine the relative differences in bacterial burden among groups of mice, because we could not determine the number of cells present in each sample. The results were considered negative for ehrlichia DNA if $C_T \geq 40$ in the PCR reaction.

RT-PCR and Quantitative Real-Time PCR Analysis of Host Genes

The mRNA from the liver samples was extracted using TRIzol reagent (Invitrogen; Life Technologies), and the cDNA was synthesized using an SA Biosciences reverse transcriptase ($RT)^2$ first-strand kit (Qiagen, Valencia, CA). The expression of IFN-I, caspase-1 and IL-1β mRNA was measured using the following primers: mIFN-α forward, 5′-AGGACAGGAAGGACTTCGGA-3′ (20 bp); mIFN-α reverse, 5′-GAGAGGTGCAGTGTCCTAGT-3′ (20 bp); caspase-1 forward, 5′-ATCATTTCCGCGGTTGAAT-3′ (19 bp); caspase-1 reverse, 5′-AATTGCTGTGTGCGCATGT-3′ (19 bp); IL-1β forward, 5′-ACCCTGCAGTGGTTCGAG-3′ (18 bp); IL-1β reverse, 5′-TTGCACAAGGAAGCTTGG-3′ (18 bp); GAPDH forward, 5′-AAATGAGAGAGGCCCAGCTA-3′ (20 bp); and GAPDH reverse, 5′-CCGCCCTGCTTATCCAGT-3′ (18 bp). The relative quantification of each gene transcript was normalized to GAPDH and, compared with that expressed in naïve mice. Quantitative real-time PCR using an RT^2 profiler PCR array kit (Qiagen) was performed for groups of genes, including *Nlrp1*, *Nlrp3*, caspase-1 (*Casp1*), caspase-11 (*Casp11*), IL-1α (*Il1a*), IL-1β (*Il1b*), and IFN-β (*Ifnb1*). cDNA samples were run on an ABI Prism 7000 sequence detection system (Life Technologies). The expression levels of approximately 200 genes were determined using SA Bioscience Pathway Finder RT^2 Profiler PCR arrays according to the manufacturer's recommendations (Qiagen). Data were collected using an ABI 7900 HT real-time PCR system (Life Technologies). The array plate contained five housekeeping genes, including *Gapdh* and β-actin (*Actb*), and one set for genomic DNA contamination as the reference genes and a control. Comparative threshold cycle values were analyzed using the manufacturer's software, and fold regulation values were plotted. The fold regulation values were calculated by

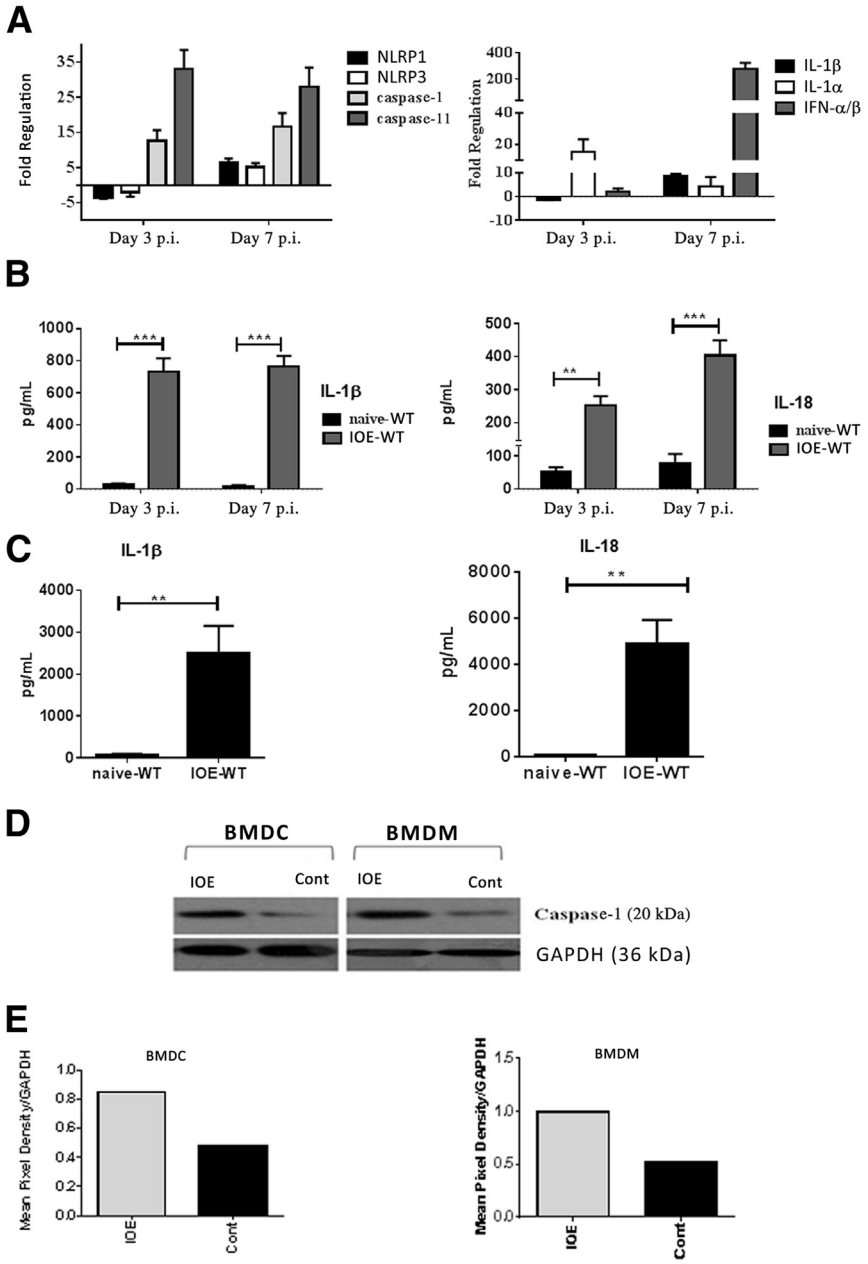

Figure 1 Lethal ehrlichial infection differentially activates inflammasomes, compared with uninfected control. **A:** Mice infected with the lethal dose of *Ixodes ovatus Ehrlichia* (IOE) had a higher mRNA expression of inflammasome components NLRP1, NLRP3, caspase-1, caspase-11, IL-1α, IL-β, and cytokine IFN-α/β in liver at different time points after infection, compared with control. Results were normalized to housekeeping genes and expressed as fold regulation, compared with gene expression in naïve mice. **B:** Levels of IL-1β and IL-18 increased in spleen of lethally IOE-infected WT mice, compared with uninfected sham controls on days 3 and 7 after infection (p.i.). **C:** Levels of IL-1β and IL-18 increased in serum of lethally IOE-infected WT mice, compared with uninfected sham controls on day 7 p.i. **D:** Western blot analysis indicated higher expression of active caspase-1 (p20) in bone marrow–derived dendritic cells (BMDCs) and bone marrow derived–macrophages (BMDMs), either infected *in vitro* with IOE or left uninfected (control). **E:** Mean pixel density of Western blotting bands for active caspase-1 was determined by ImageJ software. Data are expressed as means ± SD. $n = 9$ mice per group (**A**–**C**), pooled from two independent experiments. Western blot results (**D** and **E**) represent one of three independent experiments with similar results. $^{**}P \leq 0.01$, $^{***}P \leq 0.001$. Cont, control.

dividing the expression fold changes of the candidate genes by the expression fold changes of the reference genes using the comparative threshold cycle method. Up-regulation or down-regulation of the host genes was determined relative to naïve mice. Using cutoff criteria, fivefold up-regulation or down-regulation was considered to be significant and of biological importance.

Western Blot Analysis

Liver tissues and bone marrow–derived macrophages (BMDMs) were lysed in 1× lysis buffer (T-PER) and radioimmunoprecipitation assay buffer (Thermo Fisher Scientific, Waltham, MA), respectively, and debris was removed by centrifugation. Lysates were resolved in 4% to 20% gradient SDS–PAGE gels. The protein content of the entire gel was then transferred to a polyvinylidene difluoride membrane. The membranes were processed and probed with the following antibodies, according to standard protocols: anti–caspase-1 (2 μg/mL) (EMD Millipore, Billerica, MA); anti–caspase-11 (5 μg/mL) (Sigma-Aldrich, St. Louis, MO); anti–IL-1β (2 μg/mL) (GeneTex, Irvine, CA); anti-LC3B (dilution 1:2500) (Novus Biologicals, Littleton, CO); anti–beclin-1 (dilution 1:1000) (Cell Signaling Technology, Danvers, MA); anti-FOXP3 (dilution 1:500) (Sigma-Aldrich); and anti-GAPDH (0.2 μg/mL) (Sigma-Aldrich). Mean pixel density of bands in Western blots was determined using ImageJ software version 1.48 (NIH, Bethesda, MD).

Preparation of Mouse BMDMs and BMDCs and Infection with Cell-Free Ehrlichiae

BMDMs and bone marrow–derived dendritic cells (BMDCs) were propagated as described previously.[37] The BM cells were cultured in complete medium supplemented with 200 U/mL recombinant granulocyte-macrophage colony-stimulating factor (GM-CSF) or 5×10^6 U/mg granulocyte colony-stimulating factor (G-CSF) (PeproTech, Rocky Hill, NJ). Cell-free *E. muris* and IOE organisms were prepared from a 90% infected macrophage cell line (DH82), as well as from infected splenocytes harvested from the IOE-infected mice on day 7 p.i. as described previously.[6] Bacteria were added to the BMDM or BMDC cultures at multiplicity of infection MOI = 5. Supernatant was collected at 12 and 24 hours after infection.

Statistical Analysis

The two-tailed *t*-test was used for comparison of mean values for two experimental groups, and a one-way analysis of variance was used for comparisons of multiple experimental groups. Data are expressed as means ± SD. $P \leq 0.001$ and 0.01 were considered highly significant; $P \leq 0.05$ was considered moderately significant.

Results

Inflammasome Activation Is Linked to the Development of Fatal *Ehrlichia*-Induced Toxic Shock

The highly virulent, LPS-negative, Gram-negative IOE strain of *Ehrlichia* causes lethal infection in WT C57BL/6 mice when administered at a high dose (10^3 bacterial genomes per mouse) via the intraperitoneal route.[5–8,45,46] We have previously demonstrated that lethal ehrlichial infection triggers excessive production of IL-18 in the liver and that the lack of IL-18R enhances resistance of IOE-infected mice to lethal ehrlichiosis.[12] These findings suggested that inflammasome activation plays a detrimental role during infection with LPS-negative ehrlichiae. In the present study, to determine the molecular pathway by which ehrlichiae trigger the inflammasomes, we examined the mRNA and protein expression of several markers of inflammasomes in the liver of WT mice infected with the lethal dose of IOE. We selected the liver as the major site of infection and pathology both clinically and in mice infected with ehrlichiae. Our present results demonstrate significant up-regulation (fivefold increase in gene expression, relative to naïve mice) of mRNA expression of NLRP3, NLRP1, caspase-1, caspase-11, IL-1β, IL-1α, and IFN-β on days 3 and 7 p.i. (Figure 1A). Consistent with mRNA expression, both spleen (Figure 1B) and serum (Figure 1C) from IOE-infected mice had higher levels of IL-1β and IL-18, compared with uninfected controls (Figure 1B). We also examined caspase-1 activation in BMDMs and BMDCs, which are the main target cells for ehrlichiae. Expression of active (cleaved) caspase-1 was higher in IOE-infected BMDMs and BMDCs from WT mice, compared with uninfected cells (Figure 1, D and E). These results suggest that ehrlichiae trigger activation of the canonical inflammasome pathway and up-regulate caspase-11 expression in the murine model of fatal *Ehrlichia*-induced toxic shock.

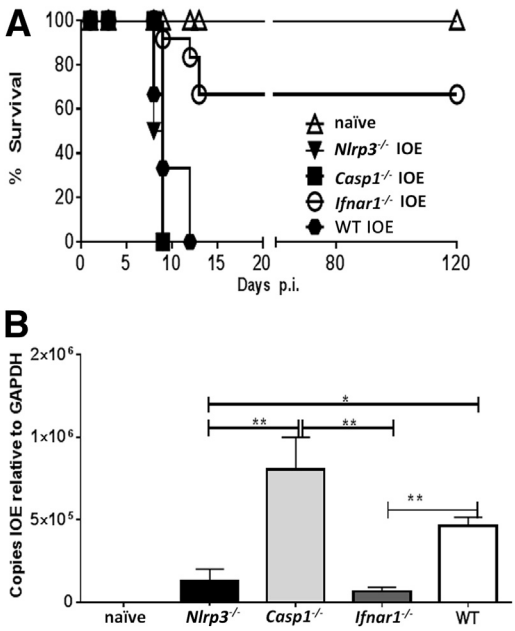

Figure 2 Enhanced resistance of *Ifnar1*$^{-/-}$ mice to lethal ehrlichiosis. **A:** Survival curves for IOE-infected mice show long-term survival of *Ifnar1*$^{-/-}$. **B:** Bacterial burden in liver of IOE-infected mice and uninfected controls was determined by quantitative real-time PCR on day 7 p.i. IOE-infected *Ifnar1*$^{-/-}$ and *Nlrp3*$^{-/-}$ mice had significantly lower bacterial burden, compared with WT and *Casp1*$^{-/-}$ mice. Data are expressed as means ± SD. $n = 12$ mice per group (**A**); $n = 9$ mice per group, pooled from three independent experiments (**B**). $^*P \leq 0.05$, $^{**}P \leq 0.01$.

Improved Survival and Protective Immunity during Ehrlichial Infection in *Ifnar1*$^{-/-}$ Mice

Recent studies have indicated that IFN-I regulate inflammasome activation during infections with intracellular pathogens.[36,42,43,47] We therefore examined IFN-I expression in a murine model of fatal ehrlichiosis. The expression of IFN-I mRNA in the liver of IOE-infected mice was approximately 150-fold higher than that detected in the uninfected controls (Figure 1A). Given that IFN-I up-regulation was associated with inflammasome activation during fatal ehrlichial infection, we hypothesized that IFN-I promotes fatal disease via activation of the inflammasome pathway. To test this hypothesis, we compared the outcome of infection in mice deficient in IFNAR1, NLRP3, or caspase-1 and infected with a high dose of IOE. We chose to further investigate the role of NLRP3 among other inflammasomes that were up-regulated during fatal ehrlichial infection (Figure 1A), to compare our model with other murine models of sepsis caused by LPS-positive, Gram-

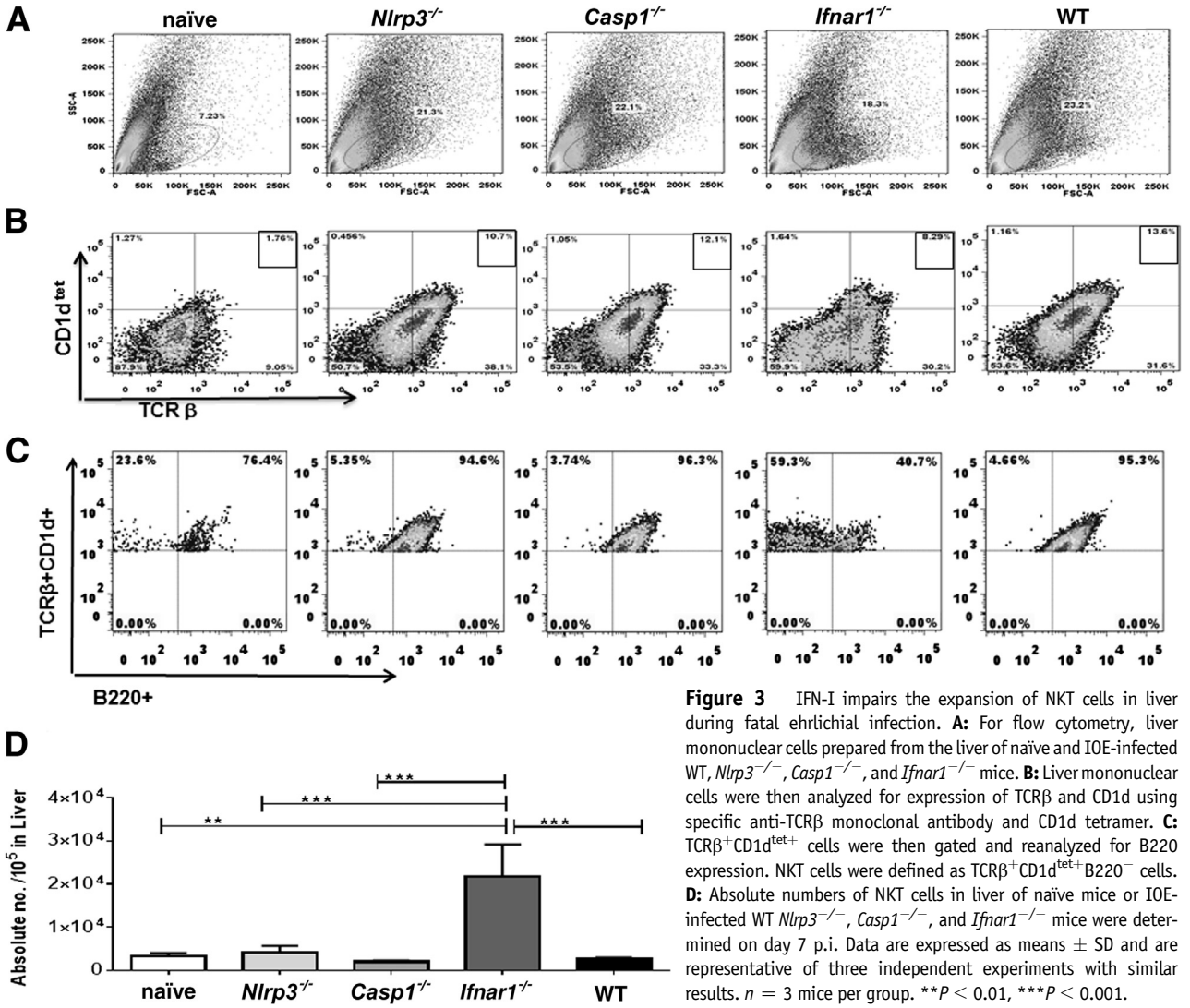

Figure 3 IFN-I impairs the expansion of NKT cells in liver during fatal ehrlichial infection. **A:** For flow cytometry, liver mononuclear cells prepared from the liver of naïve and IOE-infected WT, *Nlrp3*$^{-/-}$, *Casp1*$^{-/-}$, and *Ifnar1*$^{-/-}$ mice. **B:** Liver mononuclear cells were then analyzed for expression of TCRβ and CD1d using specific anti-TCRβ monoclonal antibody and CD1d tetramer. **C:** TCRβ^{+}CD1d^{tet+} cells were then gated and reanalyzed for B220 expression. NKT cells were defined as TCRβ^{+}CD1d^{tet+}B220^{-} cells. **D:** Absolute numbers of NKT cells in liver of naïve mice or IOE-infected WT *Nlrp3*$^{-/-}$, *Casp1*$^{-/-}$, and *Ifnar1*$^{-/-}$ mice were determined on day 7 p.i. Data are expressed as means ± SD and are representative of three independent experiments with similar results. $n = 3$ mice per group. $^{**}P \leq 0.01$, $^{***}P \leq 0.001$.

negative bacteria in which NLRP3 contributes to disease pathogenesis. Unexpectedly, 100% of *Casp1*$^{-/-}$ and *Nlrp3*$^{-/-}$ mice died of infection between days 9 and 12 p.i., a result similar to that of WT mice (Figure 2A). By contrast, approximately 75% of the IOE-infected *Ifnar1*$^{-/-}$ mice survived lethal infection past day 120 p.i (Figure 2A).

Next, we examined the contribution of the IFN-I, NLRP3 inflammasome, and caspase-1 in host defense against ehrlichiae. Our results indicated that *Casp1*$^{-/-}$ mice have a higher bacterial burden in the liver than do WT mice. Interestingly, both *Ifnar1*$^{-/-}$ and *Nlrp3*$^{-/-}$ mice had a lower bacterial burden than did WT and *Casp1*$^{-/-}$ mice (Figure 2B). These results suggest that IFNAR1 and NLRP3 signaling impairs protective immunity against ehrlichiae, independent of caspase-1 activation.

We have previously reported that protective immunity against ehrlichiae is mediated by IFN-γ–producing T cells and natural killer T cells (NKT cells).[9–11,18] However, these cells undergo apoptosis and are functionally suppressed during fatal ehrlichiosis.[5–8,10,18] We therefore tested the hypothesis that IFNAR1 and NLRP3 negatively regulate protective immune responses against ehrlichiae by NKT cells and Type I T cells. We first measured the numbers of NKT cells in the liver of different groups using CD1d-αGalCer tetramers.[18,48,49] Interestingly, *Ifnar1*$^{-/-}$, but not *Nlrp3*$^{-/-}$, mice had significantly increased percentages (Figure 3, A–C) and absolute numbers (Figure 3D) of hepatic CD1d-αGalCer tetramer–positive NKT cells (TCRβ^{+}/CD1d^{+}/B220^{-} cells), compared with IOE-infected WT and *Casp1*$^{-/-}$ mice. These results suggest that IFNAR1, but not NLRP3, inhibits the expansion or influx of protective NKT cells at the sites of infections during fatal ehrlichiosis.

Next, we examined T-cell responses in the experimental groups of mice. The *Ifnar1*$^{-/-}$ mice had significantly higher numbers of CD4^{+} T cells in spleen (Figure 4, A and C) and liver (Figure 4, B and D) on day 7 p.i., compared with all other groups of mice. In addition, *Ifnar1*$^{-/-}$ mice had significantly higher percentages (Figure 5A) and absolute numbers (Figure 5B) of IFN-γ–producing splenic CD3^{+} T cells. The increase in numbers of CD4^{+} T cells in IOE-infected *Ifnar1*$^{-/-}$ mice was not due to differences in T-cell population in *Ifnar1*$^{-/-}$ naïve mice; we did not

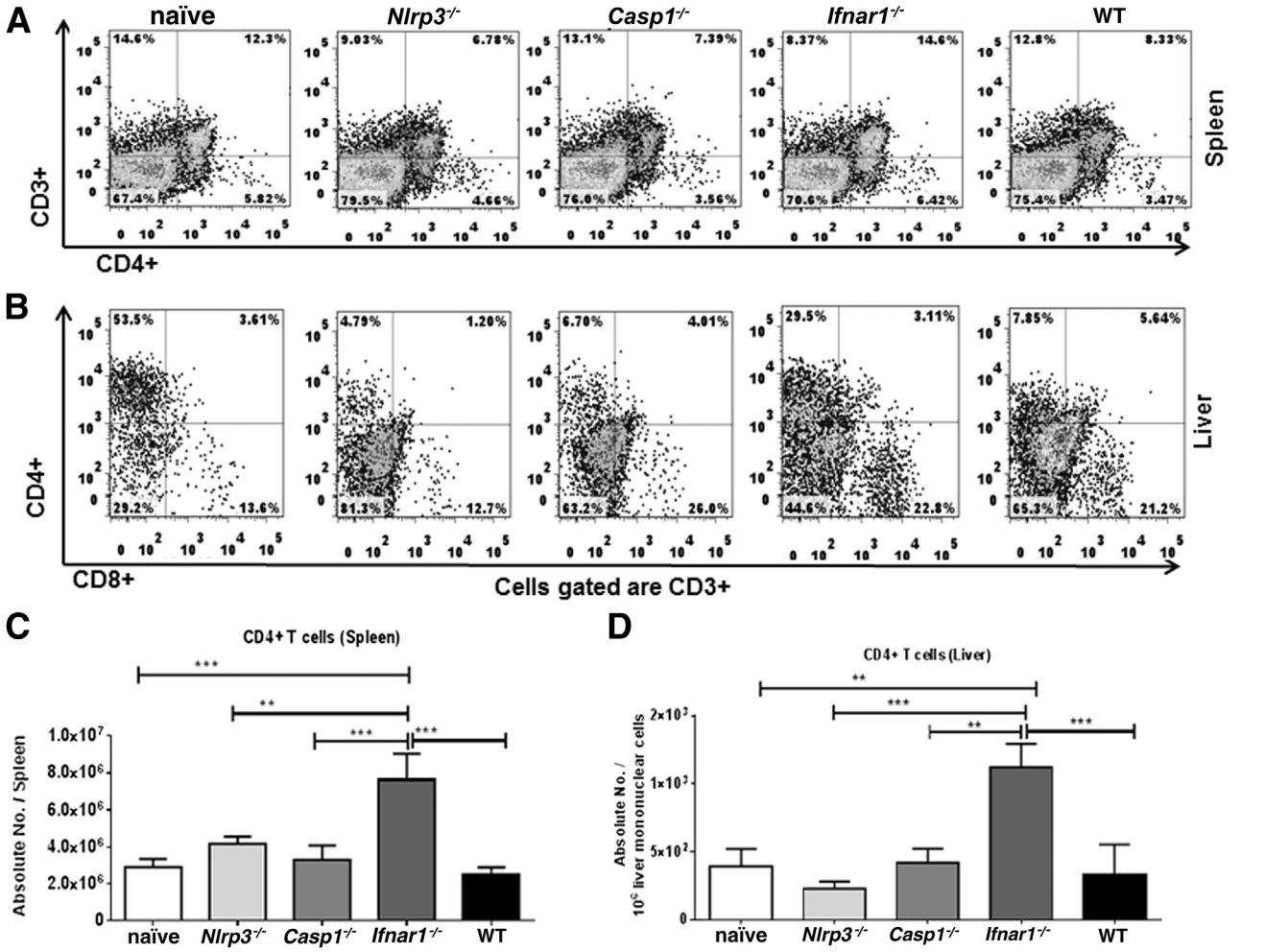

Figure 4 Expansion of the CD4$^+$ T-cell subset in *Ifnar1*$^{-/-}$ mice after lethal IOE infection. **A** and **B:** Flow cytometry analysis of the percentage of CD4$^+$ T cells in spleen (**A**) and liver (**B**) of mice on day 7 p.i. with lethal *Ixodes ovatus Ehrlichia* infection. **C** and **D:** Absolute numbers of CD4$^+$ T cells in spleen (**C**) and liver (**D**) of the same mice. Data are expressed as means ± SD, and are representative of three independent experiments with similar results. $n = 9$ mice per group. $^{**}P \leq 0.01$, $^{***}P \leq 0.001$.

detect significant changes in the numbers of different T-cell subsets among naïve mice from different backgrounds (Figure 5C). Importantly, increased frequency of Type I T cells in *Ifnar1*$^{-/-}$ mice was associated with higher IFN-γ levels, but lower IL-10 levels, in serum (Figure 6A) and spleen (Figure 6B), and therefore a lower IL-10/IFN-γ ratio (Figure 6, A and B), compared with WT and *Casp1*$^{-/-}$ mice. Although IFN-γ–producing T cells numbers in *Nlrp3*$^{-/-}$ mice did not differ significantly, compared with WT and *Casp1*$^{-/-}$ mice, the *Nlrp3*$^{-/-}$ mice had significantly higher levels of IFN-γ and had lower IL-10/IFN-γ ratios in serum (Figure 6A) and spleen (Figure 6B), compared with WT and *Casp1*$^{-/-}$ mice. These results suggest that lack of IFNAR1 and NLRP3 signaling attenuates IL-10–mediated suppressive immune responses against ehrlichiae, which may account for enhanced bacterial clearance in *Ifnar1*$^{-/-}$ and *Nlrp3*$^{-/-}$ mice.

We next examined whether enhanced protective immunity and IFN-γ production in *Ifnar1*$^{-/-}$ and *Nlrp3*$^{-/-}$ mice is due to decreased production of IL-10 by T cells, including T regulatory cells (Tregs). Tregs are known to suppress protective CD4$^+$ Th1 responses during infection with intracellular bacteria.[6,7,50,51] IOE-infected *Ifnar1*$^{-/-}$ mice had significantly lower percentages (Figure 7A) and absolute numbers of splenic IL-10–producing CD3$^+$CD4$^+$CD25$^+$ T cells in spleen, compared with the other groups (Figure 7, B and C).

To determine whether IFNAR1 signaling influences the induction of Treg cells at a primary sites of infection, we analyzed FOXP3 expression in liver tissue lysate from all groups by Western blotting, and the frequency of FOXP3–expressing Treg cells in spleen by flow cytometry. Interestingly, liver lysate from naïve mice and from IOE-infected WT, *Nlrp3*$^{-/-}$, and *Casp1*$^{-/-}$ mice expressed FOXP3 on day 7 p.i. (Figure 7D), whereas absence of IFNAR1 signaling abrogated hepatic FOXP3 expression in *Ifnar1*$^{-/-}$ mice. Similarly, IOE-infected *Ifnar1*$^{-/-}$ mice had significantly lower percentages and absolute numbers of splenic CD4$^+$FOXP3$^+$ Tregs (mainly those that express the CD25 marker), compared with

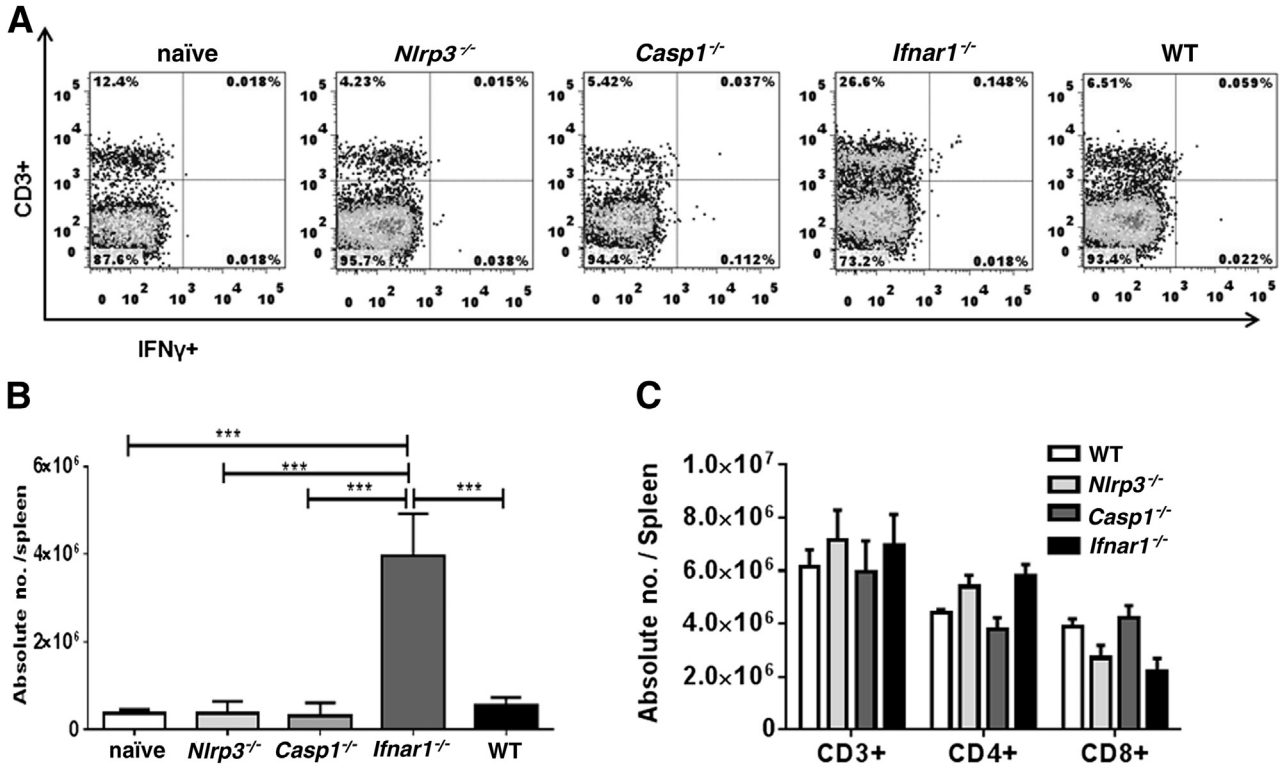

Figure 5 Enhanced protective type I immune responses in IOE-infected *Ifnar1*$^{-/-}$ mice. **A** and **B:** Flow cytometry analysis of the percentage (**A**) and absolute number (**B**) of intracellular IFN-γ—expressing CD3$^+$ splenocytes from IOE-infected WT, *Ifnar1*$^{-/-}$, *Nlrp3*$^{-/-}$, and *Casp1*$^{-/-}$ mice on day 7 p.i. **C:** Flow cytometry analysis of the absolute numbers of CD3$^+$, CD4$^+$, and CD8$^+$ T cells shows similar number of these T-cell subsets in naïve mice of different backgrounds (WT, *Ifnar1*$^{-/-}$, *Nlrp3*$^{-/-}$, and *Casp1*$^{-/-}$). Data are expressed as means ± SD and are representative of three independent experiments ($N = 9$ mice). ***$P \leq 0.001$.

IOE-infected WT and *Casp1*$^{-/-}$ mice, (Figure 8, A and B). Intriguingly, IOE-infected *Nlrp3*$^{-/-}$ mice also had significantly lower numbers of splenic CD4$^+$ CD25$^+$FOXP3$^+$ Tregs and CD4$^+$CD25$^-$FOXP3$^+$ Tregs, compared with WT and *Casp1*$^{-/-}$ mice (Figure 8, A and B). Taken together, these results suggest that IFNAR1 and NLRP3 promote both expansion of FOXP3$^+$ Tregs and production of IL-10, which may account for suppressed anti-ehrlichial immunity during fatal ehrlichiosis. Furthermore, these results show for the first time that IFNAR1 signaling is the major regulatory mechanism that controls induction of Tregs in nonlymphoid peripheral organ such as liver.

Attenuated Liver Pathology and Host Cell Death After *Ehrlichia* Infection in *Ifnar1*$^{-/-}$ Mice

The lack of correlation between the lower bacterial burden and survival in *Nlrp3*$^{-/-}$ mice suggested that fatal ehrlichial infection was not due to an overwhelming infection, but rather due to an immunopathology. This conclusion is consistent with findings from our previous studies in murine models of ehrlichiosis and in patients with human monocytotropic ehrlichiosis. We therefore evaluated the degree of liver damage in experimental groups of mice by hematoxylin and eosin and TUNEL staining. Consistent with our previous findings,[5–11,13,14,45,46] IOE-infected WT mice exhibited focal areas of confluent necrosis (Figure 9A) and extensive apoptosis of both Kupffer cells and hepatocytes (Figure 9, B and C), as well as microvesicular steatosis (Figure 9D) and congestion on days 7 to 10 p.i. Although IOE-infected *Nlrp3*$^{-/-}$ mice were able to clear ehrlichiae, these mice had focal areas of hepatocyte apoptosis and necrosis in the liver on day 7 p.i., similar to that detected in the liver of IOE-infected WT mice (Figure 9A). *Casp1*$^{-/-}$ mice had substantial foci of hepatic necrosis and significantly higher numbers of apoptotic cells than the other groups (Figure 9, B and C). By contrast, the severity of liver damage was significantly attenuated in IOE-infected *Ifnar1*$^{-/-}$ mice, as indicated by a significant decrease in the numbers of apoptotic Kupffer cells and hepatocytes ($P < 0.01$) (Figure 9, B and C). Decreased cell death in *Ifnar1*$^{-/-}$ mice was associated with more portal tract and lobular cellular infiltration (predominantly lymphocytes) and less microvesicular steatosis and congestion, compared with WT mice (data not shown). Interestingly, IOE-infected *Ifnar1*$^{-/-}$ mice showed more evidence of hepatocyte regeneration,[52] including binucleation of hepatocytes and extramedullary hematopoiesis (Figure 9E). By day 10 p.i., the majority of WT mice had died of infection, so histological assessment of WT mice was not feasible for this time point. However, *Ifnar1*$^{-/-}$ mice were all still alive at day 10 p.i. and exhibited perivascular granuloma-like lymphohistiocytic

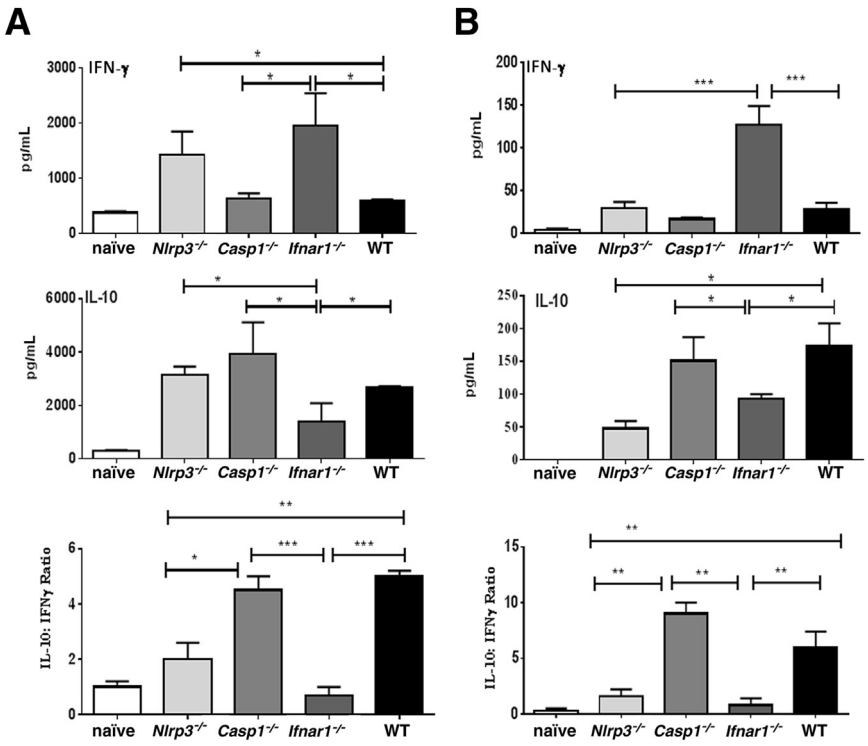

Figure 6 IFNAR1 inhibits splenic and systemic IFN-γ production while enhancing IL-10 secretion during fatal ehrlichial infection. **A:** Levels of IFN-γ and IL-10 and the ratio of IL-10 to IFN-γ in serum from all infected groups of mice at day 7 p.i. **B:** Levels of IFN-γ and IL-10 and the IL-10/ IFN-γ ratio in culture supernatants from spleen harvested from all infected groups of mice on day 7 p.i. Data are expressed as means ± SD and are representative of three independent experiments with similar results. $n = 9$ mice per group. $^{*}P \leq 0.05$, $^{**}P \leq 0.01$, and $^{***}P \leq 0.001$.

infiltrates in the liver (Figure 9E), a result similar to those previously reported in the murine model of mild ehrlichiosis.[6] Our previous studies indicated that ehrlichiae-induced granuloma formation is a marker of protective cell-mediated immunity against intracellular ehrlichiae.[51,53] *Ifnar1*$^{-/-}$ mice also exhibited evidence of resolving liver injury (eg, less confluent necrosis) at day 10 p.i. (Figure 9F). Thus, IFNAR1 signaling promotes severe liver damage in the murine model of fatal ehrlichiosis via a pathway that is independent of the caspase-1 and the NLRP3 inflammasomes. The lack of correlation between bacterial burden and pathology in IOE-infected *Nlrp3*$^{-/-}$ mice further suggests that fatal ehrlichiosis is due to immune-mediated pathology, rather than to overwhelming infection.

IFNAR1 Regulates Noncanonical Inflammasome Activation during Fatal *Ehrlichia* Infection

The results described above suggested that detrimental inflammasome activation in the murine model of fatal ehrlichiosis is not mediated by caspase-1 (the canonical inflammasome pathway). The activation of caspase-11 via the noncanonical inflammasome pathway mediates inflammatory host-cell death and secretion of IL-1β.[54–56] We hypothesized that IFN-I mediates the activation of caspase-11 and triggers the noncanonical inflammasome pathway, causing excessive inflammation and tissue injury after lethal ehrlichial infection. To test our hypothesis, we first measured IL-1β secretion in all groups of mice. Compared with WT and *Casp1*$^{-/-}$ mice, the level of the biologically active form of IL-1β (17 kDa) was significantly decreased in liver lysate (Figure 10A) and serum (Figure 10B) from *Ifnar1*$^{-/-}$ and *Nlrp3*$^{-/-}$ mice on day 7 p.i. Surprisingly, *Casp1*$^{-/-}$ mice still produced significant levels of IL-1β in liver and serum, compared with uninfected controls (Figure 10, A and B). These results suggest that IL-1β secretion in the murine model of fatal ehrlichiosis is dependent on IFNAR1, and partially dependent on NLRP3, but independent of caspase-1.

Next, we measured the expression of active caspase-11 in liver lysate of IOE-infected mice on day 7 p.i. Active caspase-11 was highly expressed in the liver of WT and *Casp1*$^{-/-}$ mice, whereas it was partially decreased in the liver lysate from *Nlrp3*$^{-/-}$ mice. By contrast, expression of active caspase-11 in the liver of *Ifnar1*$^{-/-}$ was completely abrogated (Figure 10A). These results suggest that ehrlichiae induce activation of the noncanonical inflammasome pathway *in vivo*, which is completely dependent on IFNAR1 and is mediated in part by NLRP3 signaling. *In vitro* results also showed that expression of pro–caspase-11 and active caspase-11 in BMDMs is dependent on IFNAR1, as evidenced by decreased expression of pro–caspase-11 in IOE-infected BMDMs from *Ifnar1*$^{-/-}$ mice, compared with WT mice (Figure 10, C and D). Of note, we did not detect cleavage and activation of caspase-11 in IOE-infected WT or *Ifnar1*$^{-/-}$ BMDMs (data not shown), suggesting that *in vitro* IOE-infected BMDMs lack danger signaling mechanisms that promote activation and cleavage of caspase-11. In accord with other reports, we did not detect expression of pro–caspase-11 or active caspase-11 in uninfected or IOE-infected BMDMs or BMDCs from *Casp1*$^{-/-}$ mice (data not shown). Surprisingly, active caspase-11 was also expressed in liver lysate from IOE-infected *Casp1*$^{-/-}$ mice (Figure 10A). These results

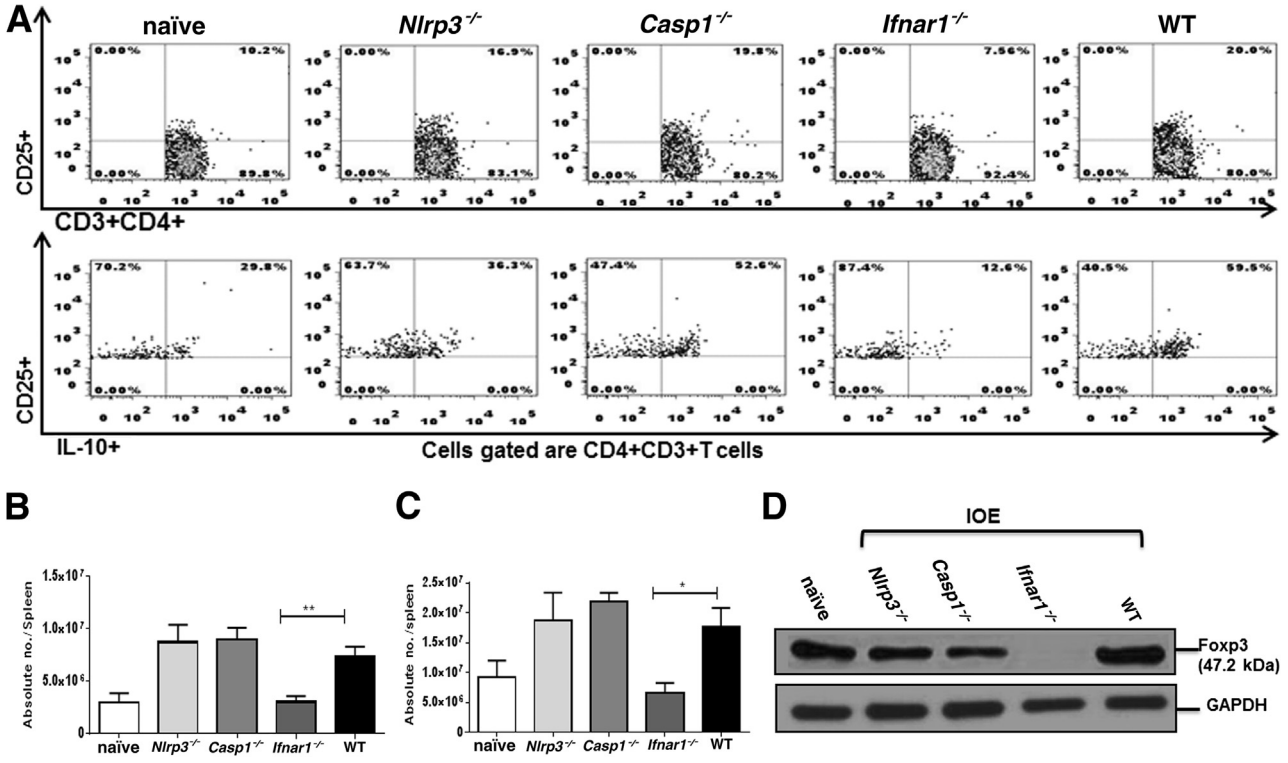

Figure 7 IFNAR1 signaling increased the numbers of IL-10—producing-$CD3^+CD4^+CD25^+$ T cells and the number of FOXP3-expressing Tregs in liver during fatal ehrlichial infection. **A:** Flow cytometry analysis of the percentage of $CD3^+CD4^+CD25^+$ and IL-$10^+CD3^+CD4^+CD25^+$ T cells in spleen at day 7 p.i. **B** and **C:** Absolute number of $CD3^+CD4^+CD25^+$ T cells (**B**) and IL-$10^+CD3^+CD4^+CD25^+$ T cells (**C**) in spleen at day 7 p.i. **D:** FOXP3 protein expression in liver was determined via Western blot analysis of liver lysate. Data are expressed as means ± SD and are representative of three independent experiments with similar results. $n = 9$ mice per group. $^*P \leq 0.05$, $^{**}P \leq 0.01$.

suggest that caspase-11 expression and activation is induced in the liver of *Casp1*$^{-/-}$ mice on ehrlichial infection.

Ehrlichiae Block Autophagy Processing That Is Dependent on IFNAR1

Previous studies have shown that inhibition of inflammasome activation after infection with LPS-positive, Gram-negative bacteria augments the autophagy flux.[33,57–66] Autophagy is also an important host defense mechanism that mediates clearance of intracellular bacteria. We therefore hypothesized that IFNAR1 mediates inflammmasome activation in IOE-infected WT and other susceptible mice (*Casp1*$^{-/-}$ and *Nlrp3*$^{-/-}$), which in turn inhibits the autophagocytic response to ehrlichiae. To test this hypothesis, we examined the difference in autophagosome processing marked by LC3 in all groups of mice. Two forms of LC3 (ie, LC3I and LC3II) are produced post-translationally. LC3I is cytosolic, whereas LC3II is membrane bound and exhibits enrichment on the autophagosome vacuoles.[19,67] The LC3 processing indicated by a higher LC3II/LC3I ratio suggests effective autophagy flux whereby the autophagosome fuses with the lysosome, leading to the degradation of intracellular bacteria. Our results demonstrated that the high susceptibility of IOE-infected WT and *Casp1*$^{-/-}$ mice is associated with equal expression of both LC3I and LC3II in liver lysate (Figure 11, A and B), which suggests defective autophagosome processing. By contrast, liver lysate from IOE-infected *Ifnar1*$^{-/-}$ and *Nlrp3*$^{-/-}$ mice had three- and fourfold higher expression of LC3II than LC3I, respectively, which suggests LC3 processing (Figure 11, A and B). However, the level of both forms of LC3 was lower in IOE-infected *Ifnar1*$^{-/-}$ mice than in the other groups of mice. Because *Ifnar1*$^{-/-}$ mice were able to effectively clear ehrlichiae, we postulated that low levels of LC3II could be due to enhanced autophagy flux and binding of the autophagosome to the lysosome.

To further determine whether the lack of LC3 processing is coupled with defective induction of the autophagosome in IOE-infected WT and *Casp1*$^{-/-}$ mice, compared with *Nlrp3*$^{-/-}$ and *Ifnar1*$^{-/-}$ mice, we examined beclin-1 expression in liver lysate. Beclin-1 is an important protein that mediates autophagy initiation and nucleation, and its function is thought to be controlled by cleavage.[58,68] The WT mice and all knockout mice expressed similar levels of full-length beclin-1 in the liver tissues on day 7 p.i. (Figure 11, A and C). However, cleaved beclin-1 was detected in liver lysate of IOE-infected WT, *Casp1*$^{-/-}$, and *Nlrp3*$^{-/-}$ mice, but not *Ifnar1*$^{-/-}$ mice (Figure 11, A and C). Studies have indicated that cleaved beclin-1 fails to induce autophagy but can associate with mitochondria to induce apoptosis.[68,69] In conclusion, the correlation between ineffective bacterial

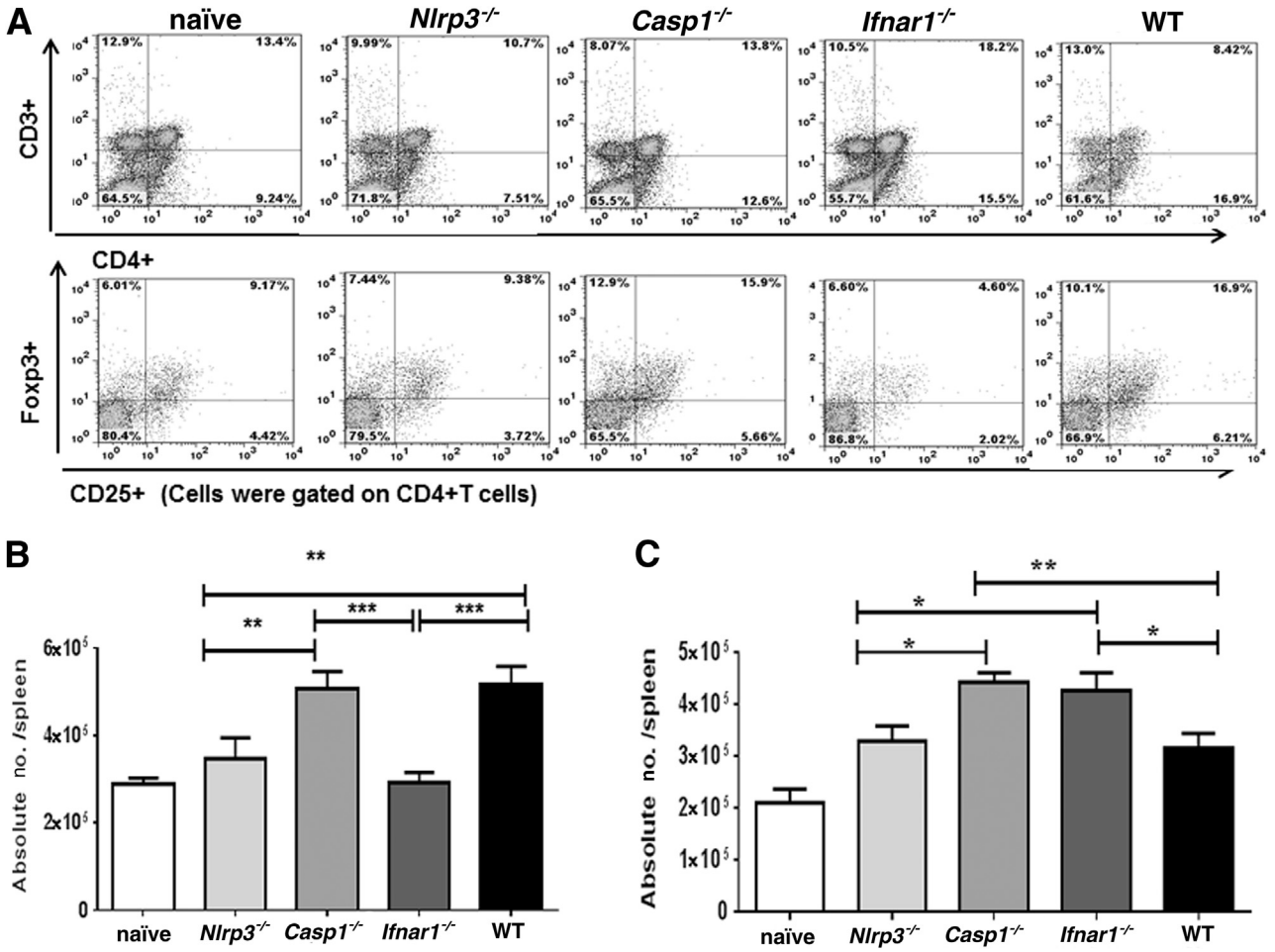

Figure 8 IFNAR1 signaling promotes expansion of FOXP3$^+$ Treg cells in spleen during fatal ehrlichial infection. **A:** Flow cytometry analysis of the percentage of CD3$^+$CD4$^+$CD25$^+$FOXP3$^+$ Tregs. **B** and **C:** Absolute number of CD4$^+$CD25$^+$FOXP3$^+$ (**B**) and of CD3$^+$CD4$^+$CD25$^-$FOXP3$^+$ (**C**) Tregs in spleen of the different groups, including uninfected control, at day 7 p.i. Data are expressed as means ± SD and are representative of two independent experiments with similar results. $n = 9$ mice per group. $^*P \leq 0.05$, $^{**}P \leq 0.01$, and $^{***}P \leq 0.001$.

clearance in WT and *Casp1*$^{-/-}$ mice, compared with *Nlrp3*$^{-/-}$ and *Ifnar1*$^{-/-}$ mice, suggests that autophagy is blocked during fatal ehrlichial infection via a pathway that is dependent on NLRP3 and IFNAR1 signaling.

Discussion

We have previously demonstrated that inflammasome activation plays a detrimental role in the pathogenesis of *Ehrlichia*-induced toxic shock.[12] With the present study, we have demonstrated that IFNAR1 contributes to caspase-11–mediated, noncanonical inflammasome activation and the subsequent secretion of the caspase-1–dependent cytokine IL-1β, thus promoting host susceptibility to fatal ehrlichial infection. In addition, our results suggest that NLRP3 and caspase-1 are involved in the secretion of IL-1β and inflammasome activation in response to ehrlichiae, although these pathways play a minor role in host susceptibility to fatal ehrlichial infection. A recent study has indicated that IFN-I promotes severe disease in the murine model of fatal ehrlichiosis,[43] although a clear mechanism has not been identified. Our results indicate that IFNAR1 impairs protective immunity while enhancing host-cell death and immunopathology, and that both mechanisms are essential determinants of disease progression and the development of multiorgan failure after fatal ehrlichial infection.

We and others have demonstrated that the effective clearance of ehrlichiae is mediated by the balance between the protective responses mediated by IFN-γ, NKT cells and CD4$^+$ Th1 cells and the suppressive responses mediated by the IL-10 and IL-10–producing CD4$^+$ T cells.[7–12] IL-10 inhibits intracellular bacterial elimination via the suppression of IFN-γ–producing T cells and bactericidal functions of phagocytic cells.[45,46] Consistent with our previous results, in the present study responses in the murine model of fatal ehrlichiosis were biased toward a weak NKT-cell response and a suppressive T-cell phenotype. By contrast, the lack of IFNAR1 restored the protective phenotype. More importantly, the lack of IFNAR1 abrogated local and systemic IL-10 production and expansion of IL-10–producing

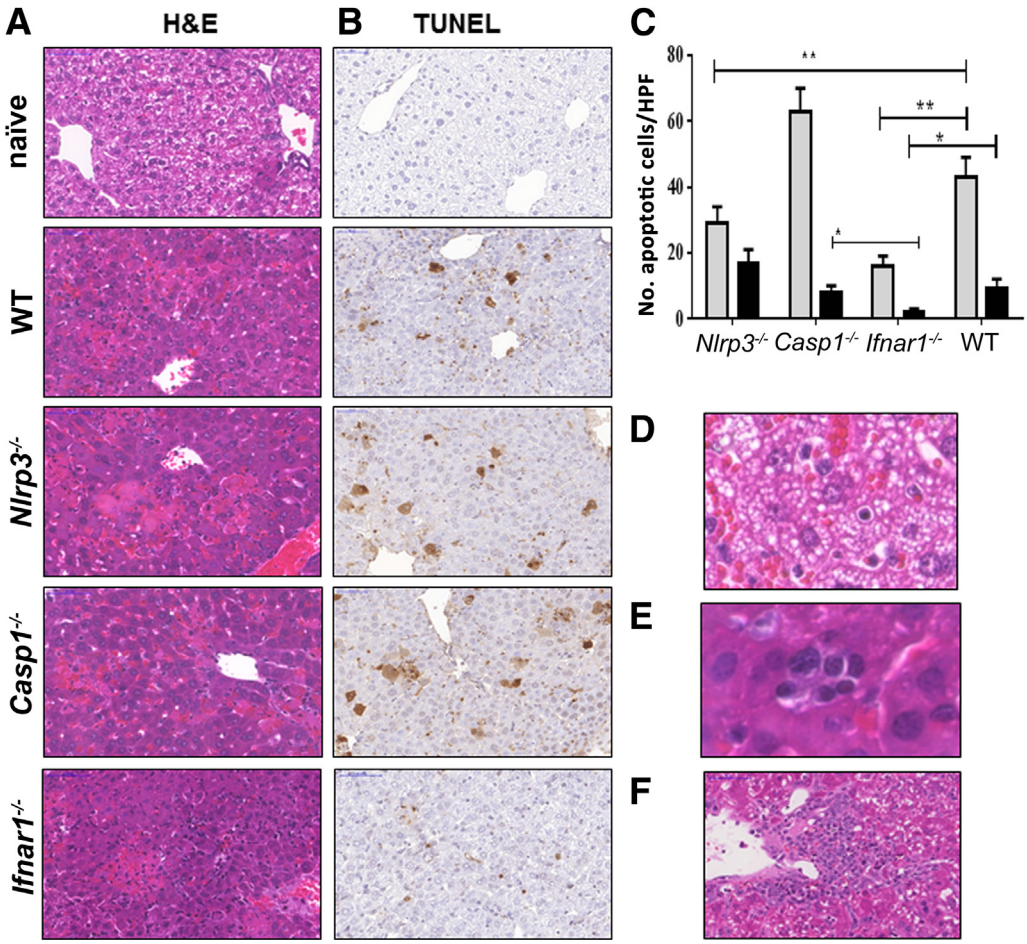

Figure 9 IOE-infected *Ifnar1*$^{-/-}$ mice have altered hepatic pathology, with increased cellular infiltration and less apoptosis, compared with WT mice. **A** and **B:** Livers were harvested on day 7 p.i., and liver sections were stained by hematoxylin and eosin (H&E) (**A**) or by TUNEL (**B**). **C:** Tunel assay revealed significantly lower numbers of apoptotic Kupffer cells (gray bars, $P < 0.01$) and hepatocytes (black bars, $P < 0.01$) in IFNaR1$^{-/-}$ mice, compared with WT and casp1$^{-/-}$ mice. The number of apoptotic Kupffer cells, but not hepatocytes, in NLRP3$^{-/-}$ mice was also significantly lower than that detected in WT and casp1$^{-/-}$ mice. The number of apoptotic cells was counted within 10 high-power fields (×40 magnification). **D:** Liver from IOE-infected WT mice, but not *Ifnar1*$^{-/-}$ mice, exhibited microvesicular steatosis. **E:** Compared with the other groups, liver of IOE-infected *Ifnar1*$^{-/-}$ mice had more inflammatory cell infiltration (composed primarily of lymphocytes) and pronounced regenerative changes, including extramedullary hematopoiesis with aggregates of erythrocyte precursors observed within sinusoids. **F:** By day 10 p.i., when most WT mice had died of infection, *Ifnar1*$^{-/-}$ mice exhibited prominent perivascular granuloma-like lymphohistiocytic infiltrates. Data are expressed as means ± SD and are representative of three independent experiments with similar results. $n = 9$ mice per group. *$P \leq 0.05$, **$P \leq 0.01$. Original magnification, ×40. HPF, high-power field.

CD4$^+$ T cells and FOXP3$^+$CD25$^+$ Tregs at secondary lymphoid organs (spleen), as well as FOXP3$^+$ Tregs at peripheral sites of infection (liver) (Figures 7D and 8, A–C), which restores the protective Th1 response against ehrlichiae. These intriguing results show a correlation between the immune regulatory responses in peripheral organs (liver) and secondary lymphoid organs (spleen). In addition, our results reveal for the first time that activation of IFN-I is the major mechanism that accounts for induction and/or expansion of FOXP3$^+$ Tregs at the site of infection and is responsible for suppression of protective immunity during infection with these obligate intracellular bacteria.

Our present results explain the recent finding that IFN-γ neutralization in IOE-infected *Ifnar1*$^{-/-}$ mice fails to revert the protective immune phenotype observed in these knockout mice.[43] Decreased IL-10 production, decreased frequency of FOXP3$^+$ Tregs at lymphoid and peripheral organs, and increased expansion of NKT cells observed in IOE-infected *Ifnar1*$^{-/-}$ mice are the likely factors that provide optimal host defense and protective immunity in our model. In support of this conclusion, in the present study IOE-infected *Nlrp3*$^{-/-}$ mice were able to clear infection similar to *Ifnar1*$^{-/-}$ mice, even though neither IFN-γ production nor IFN-γ–producing cell numbers increased in the absence of NLRP3 signaling. However, effective bacterial clearance in *Nlrp3*$^{-/-}$ mice correlated with decreased production of IL-10 and decreased numbers of FOXP3$^+$CD25$^+$ Tregs in spleen, which may account for enhanced bacterial clearance in these mice.

Our results also suggest that the enhanced intracellular bacterial elimination in *Nlrp3*$^{-/-}$ and *Ifnar1*$^{-/-}$ could be mediated also by effective autophagy flux (Figure 11).

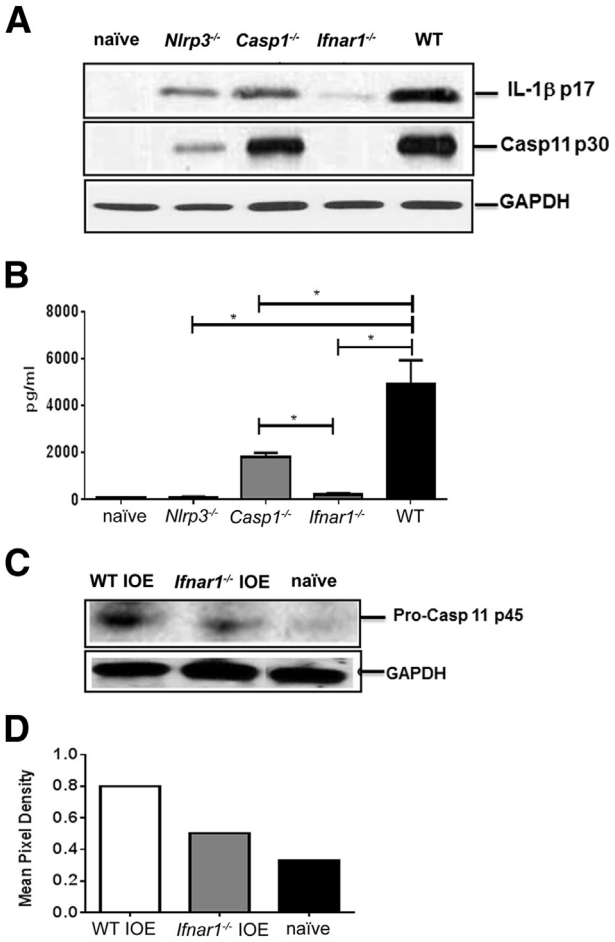

Figure 10 IFNAR1 regulates IL-1β secretion during fatal ehrlichial infection. **A:** Liver lysate from the different groups of mice was analyzed for expression of IL-1β (p17) and active caspase-11 (p30) by Western blotting on day 7 p.i. GAPDH expression was used as loading control. **B:** Serum levels of IL-1β were measured using enzyme-linked immunosorbent assay on day 7 p.i. **C** and **D:** BMDMs from IOE-infected WT and *Ifnar1*$^{-/-}$ mice express pro—caspase-11 (p45). Expression of pro—caspase-11 was normalized to GAPDH. Results in **A**, **C**, and **D** are from one mouse in each group and are representative of three independent experiments with similar results ($n = 9$ mice per group). Data in **B** are expressed as means ± SD and are representative of three independent experiments with similar results ($n = 9$ mice per group). *$P \leq 0.05$.

Defective LC3 processing and beclin-1 cleavage fail to clear ehrlichiae in WT and *Casp1*$^{-/-}$ mice, in contrast to *Ifnar1*$^{-/-}$ and *Nlrp3*$^{-/-}$ mice (Figure 11). These results suggest that autophagy flux is blocked in the murine model of fatal ehrlichiosis via an IFNAR1-dependent mechanism. How IFNAR1 blocks autophagy during ehrlichiosis is not yet known. Several studies have demonstrated a causal relationship between activation of inflammasomes and defective autophagy process. In the present study, the correlation between decreased IL-1β secretion, lack of caspase-1 activation, effective bacterial clearance, and enhanced autophagy flux suggest a similar mechanism in fatal ehrlichiosis. This raises the question of whether autophagy occurs upstream or downstream of inflammasome activation. A recent study suggested that, during infection with Gram-negative bacteria, autophagy flux occurs as a countermeasure to reduce excessive caspase-11 activation by cytosolic LPS.[47] We argue, however, that the *Ehrlichia*-induced block in autophagy processing in WT host occurs upstream of noncanonical inflammasome activation. This conclusion is supported by several findings. First, our kinetic studies have demonstrated that ineffective elimination of ehrlichiae by innate response precedes the excessive inflammasome activation and production of inflammatory cytokines.[5–7,9–11,45,46] Second, a recent study demonstrated that *Anaplasma phagocytophilum,* obligate intracellular bacteria closely related to ehrlichiae, secrete a type IV effector (ATs-1) that hijacks the beclin-1 autophagy pathway as an immune evasion and early survival mechanism.[58] Although a similar mechanism has not yet been identified in ehrlichiae, cleavage of beclin-1 in ehrlichia-infected WT mice may be due to binding of secreted molecule or molecules to beclin-1 at an early stage of infection, causing defective autophagy (Figure 11). This in turn would lead to failure to clear microbial and host danger signals (pathogen-associated and damage-associated molecular patterns, known as PAMPs and DAMPs) that trigger inflammasome activation.

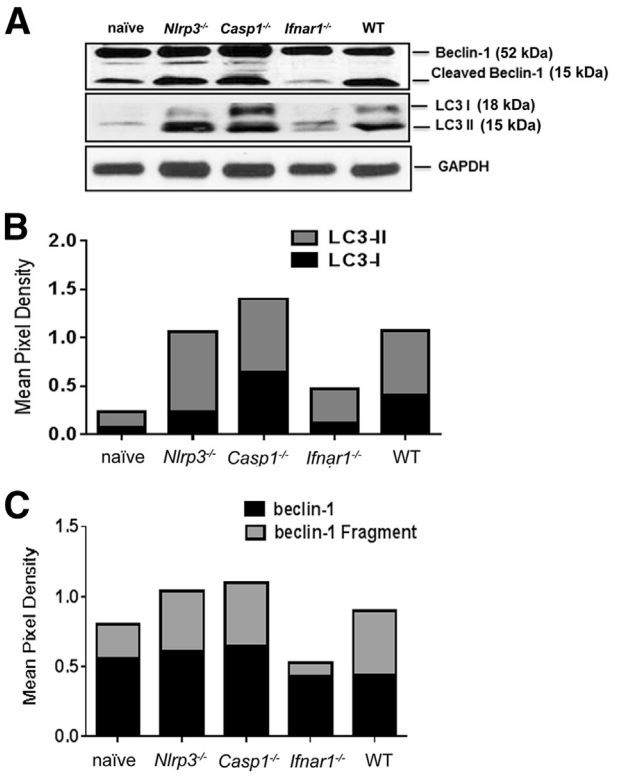

Figure 11 IFN-I blocks degradation of autophagy during fatal ehrlichial infection. Liver lysate from the different groups of mice was analyzed for expression of autophagy markers LC3I and LC3II (**A** and **B**) and beclin-1 (**A** and **C**) by Western blotting on day 7 p.i. GAPDH expression was used as loading control. Band density was quantified using ImageJ software and was normalized to GAPDH. Results are from one mouse in each group and are representative of three independent experiments with similar results. $n = 3$ mice per group.

Immunopathology, marked by host-cell apoptosis and hepatic microvesicular steatosis, is a major mechanism responsible for multiorgan failure during lethal ehrlichial infection in mice (Figure 9, A and B) and humans.[13,14,21,26,70] Both the correlation between the attenuation of pathology and host-cell death and the resistance to fatal ehrlichiosis in *Ifnar1*$^{-/-}$ mice and the lack of correlation between effective bacterial elimination and survival in *Nlrp3*$^{-/-}$ mice strongly support the conclusion that fatal ehrlichiosis is due mainly to excessive immunopathology. Activation of caspase-11 is known to trigger inflammatory host-cell death (ie, pyroptosis)[36,71,72] associated with secretion of IL-1α and IL-1β, both of which are detected in fatal ehrlichial infection (Figure 1). Abrogation of caspase-11 activation in IOE-infected *Ifnar1*$^{-/-}$ mice (Figure 10) suggests that IFNAR1 induces host-cell death during fatal ehrlichial infection via activation of the caspase-11−dependent noncanonical inflammasome pathway.

Finally, our results demonstrate that caspase-1 is dispensable for toxic shock caused by LPS-negative ehrlichiae independent of IL-1β production. The presence of overwhelming infection, extensive host-cell death, and incomplete attenuation of IL-1β secretion in IOE-infected *Casp1*$^{-/-}$ mice, compared with WT mice, suggests that other caspases may promote detrimental inflammasome activation. Caspase-8 has been demonstrated to assemble a multimeric protein complex in response to bacterial infection and to induce pro−IL-1β processing in host cells infected with pathogenic bacteria, distinct from the NLRP3−caspase-1 inflammasome pathway.[73] Other studies have indicated that caspase-11 expression increases susceptibility to *Salmonella* species infection in the absence of caspase-1[55]. We therefore speculate that the expression of caspase-8- or caspase-11−mediated processing of IL-1β and cell death in *Casp1*$^{-/-}$ mice is more apparent in the absence of caspase-1 and may account for heightened host susceptibility to fatal ehrlichial infection. The exact mechanism that accounts for the difference between our results and those described in sepsis models caused by other bacteria or acute lung injury caused by LPS injection is not yet known. However, because ehrlichiae lack LPS, we argue that *Ehrlichia*-induced IFN-1 response and inflammasome activation involve signaling by other pathogen-associated molecular patterns. For example, ehrlichiae express type IV and type I secretion systems,[4] through which several bacterial effector molecules [eg, tandem repeat protein 47 (TRP47), TRP120, TRP32, and the ankyrin repeat protein Ank200)] are secreted into the cytosol and extracellular milieu. These effectors are involved in several molecular host−pathogen interactions, including DNA binding and signaling events that lead to immune evasion, transcriptional regulation, actin nucleation, bacterial dissemination, and apoptosis.[4] Thus, these bacterial effector molecules may be major ligands that trigger inflammasome activation and IFN-1 responses in fatal ehrlichiosis, a possibility to be explored in future studies.

In summary, the present study establishes, for the first time, that IFN-I is the master regulator of the observed detrimental innate and acquired immune responses during infection with ehrlichiae, which are obligate intracellular bacteria that lack LPS. Critical mechanisms include the blocking of autophagy and the activation of the caspase-11−dependent noncanonical inflammasome pathway. By engaging caspase-11 and blocking LC3 maturation, ehrlichiae trigger host-cell death, enhance bacterial replication, and induce assembly of the NLRP3 inflammasome or of other as yet unidentified inflammasomes to activate caspase-1 activation, which (in part) mediates IL-1β/IL-18 secretion. As we have recently reported,[12] IL-18 and host-cell death induce pathogenic-acquired immune responses and bias the anti-ehrlichial T-cell responses toward the suppressive phenotype. The present results have important clinical implications and could help lead to design of novel immunotherapeutic agents that target IFN-I and/or caspase-11 pathways and thus inhibit development of dysregulated inflammation and immunopathology while promoting protective immunity against ehrlichiae or similar Gram-negative bacteria.

Acknowledgments

We thank Dr. Galina Shurin for help with preparation of single cells from mouse livers and Dr. Jake Demetris for input and help in evaluation of liver histopathology. Anti−α-GalCer−loaded CD1d tetramer was a gift from Dr. Luc Van Kaer (Vanderbilt University School of Medicine, Nashville, TN).

References

1. Olano JP, Walker DH: Human ehrlichioses. Med Clin North Am 2002, 86:375−392
2. Walker DH, Dumler JS: Human monocytic and granulocytic ehrlichioses. Discovery and diagnosis of emerging tick-borne infections and the critical role of the pathologist. Arch Pathol Lab Med 1997, 121:785−791
3. Fichtenbaum CJ, Peterson LR, Weil GJ: Ehrlichiosis presenting as a life-threatening illness with features of the toxic shock syndrome. Am J Med 1993, 95:351−357
4. Wakeel A, den Dulk-Ras A, Hooykaas PJ, McBride JW: Ehrlichia chaffeensis tandem repeat proteins and Ank200 are type 1 secretion system substrates related to the repeats-in-toxin exoprotein family. Front Cell Infect Microbiol 2011, 1:22
5. Ismail N, Crossley EC, Stevenson HL, Walker DH: Relative importance of T-cell subsets in monocytotropic ehrlichiosis: a novel effector mechanism involved in Ehrlichia-induced immunopathology in murine ehrlichiosis. Infect Immun 2007, 75:4608−4620
6. Ismail N, Soong L, McBride JW, Valbuena G, Olano JP, Feng HM, Walker DH: Overproduction of TNF-alpha by CD8+ type 1 cells and down-regulation of IFN-gamma production by CD4+ Th1 cells contribute to toxic shock-like syndrome in an animal model of fatal monocytotropic ehrlichiosis. J Immunol 2004, 172:1786−1800
7. Ismail N, Stevenson HL, Walker DH: Role of tumor necrosis factor alpha (TNF-alpha) and interleukin-10 in the pathogenesis of severe murine monocytotropic ehrlichiosis: increased resistance of TNF receptor p55- and p75-deficient mice to fatal ehrlichial infection. Infect Immun 2006, 74:1846−1856
8. Ismail N, Walker DH, Ghose P, Tang YW: Immune mediators of protective and pathogenic immune responses in patients with mild

and fatal human monocytotropic ehrlichiosis. BMC Immunol 2012, 13:26
9. Stevenson HL, Jordan JM, Peerwani Z, Wang HQ, Walker DH, Ismail N: An intradermal environment promotes a protective type-1 response against lethal systemic monocytotropic ehrlichial infection. Infect Immun 2006, 74:4856–4864
10. Stevenson HL, Estes MD, Thirumalapura NR, Walker DH, Ismail N: Natural killer cells promote tissue injury and systemic inflammatory responses during fatal Ehrlichia-induced toxic shock-like syndrome. Am J Pathol 2010, 177:766–776
11. Stevenson HL, Crossley EC, Thirumalapura N, Walker DH, Ismail N: Regulatory roles of CD1d-restricted NKT cells in the induction of toxic shock-like syndrome in an animal model of fatal ehrlichiosis. Infect Immun 2008, 76:1434–1444
12. Ghose P, Ali AQ, Fang R, Forbes D, Ballard B, Ismail N: The interaction between IL-18 and IL-18 receptor limits the magnitude of protective immunity and enhances pathogenic responses following infection with intracellular bacteria. J Immunol 2011, 187:1333–1346
13. Yang Q, Ghose P, Ismail N: Neutrophils mediate immunopathology and negatively regulate protective immune responses during fatal bacterial infection-induced toxic shock. Infect Immun 2013, 81: 1751–1763
14. Chattoraj P, Yang Q, Khandai A, Al-Hendy O, Ismail N: TLR2 and Nod2 mediate resistance or susceptibility to fatal intracellular Ehrlichia infection in murine models of ehrlichiosis. PLoS One 2013, 8: e58514
15. Vladimer GI, Marty-Roix R, Ghosh S, Weng D, Lien E: Inflammasomes and host defenses against bacterial infections. Curr Opin Microbiol 2013, 16:23–31
16. Franchi L, Núñez G: Immunology. Orchestrating inflammasomes. Science 2012, 337:1299–1300
17. Davis BK, Wen H, Ting JP: The inflammasome NLRs in immunity, inflammation, and associated diseases. Annu Rev Immunol 2011, 29: 707–735
18. Mattner J, Debord KL, Ismail N, Goff RD, Cantu C 3rd, Zhou D, Saint-Mezard P, Wang V, Gao Y, Yin N, Hoebe K, Schneewind O, Walker D, Beutler B, Teyton L, Savage PB, Bendelac A: Exogenous and endogenous glycolipid antigens activate NKT cells during microbial infections. Nature 2005, 434: 525–529
19. Liu D, Rhebergen AM, Eisenbarth SC: Licensing adaptive immunity by NOD-like receptors. Front Immunol 2013, 4:486
20. Eisenbarth SC, Williams A, Colegio OR, Meng H, Strowig T, Rongvaux A, Henao-Mejia J, Thaiss CA, Joly S, Gonzalez DG, Xu L, Zenewicz LA, Haberman AM, Elinav E, Kleinstein SH, Sutterwala FS, Flavell RA: NLRP10 is a NOD-like receptor essential to initiate adaptive immunity by dendritic cells. Nature 2012, 484: 510–513
21. Olive C: Pattern recognition receptors: sentinels in innate immunity and targets of new vaccine adjuvants. Expert Rev Vaccines 2012, 11: 237–256
22. Kumar H, Kawai T, Akira S: Pathogen recognition by the innate immune system. Int Rev Immunol 2011, 30:16–34
23. Kumar S, Ingle H, Prasad DV, Kumar H: Recognition of bacterial infection by innate immune sensors. Crit Rev Microbiol 2013, 39: 229–246
24. von Moltke J, Trinidad NJ, Moayeri M, Kintzer AF, Wang SB, van Rooijen N, Brown CR, Krantz BA, Leppla SH, Gronert K, Vance RE: Rapid induction of inflammatory lipid mediators by the inflammasome in vivo. Nature 2012, 490:107–111
25. Latz E, Xiao TS, Stutz A: Activation and regulation of the inflammasomes. Nat Rev Immunol 2013, 13:397–411
26. Franchi L, Muñoz-Planillo R, Núñez G: Sensing and reacting to microbes through the inflammasomes. Nat Immunol 2012, 13: 325–332
27. Misawa T, Takahama M, Kozaki T, Lee H, Zou J, Saitoh T, Akira S: Microtubule-driven spatial arrangement of mitochondria promotes activation of the NLRP3 inflammasome. Nat Immunol 2013, 14: 454–460
28. Franchi L, Eigenbrod T, Muñoz-Planillo R, Núñez G: The inflammasome: a caspase-1-activation platform that regulates immune responses and disease pathogenesis. Nat Immunol 2009, 10: 241–247
29. Sahoo M, Ceballos-Olvera I, del Barrio L, Re F: Role of the inflammasome, IL-1beta, and IL-18 in bacterial infections. ScientificWorldJournal 2011, 11:2037–2050
30. Rayamajhi M, Zhang Y, Miao EA: Detection of pyroptosis by measuring released lactate dehydrogenase activity. Methods Mol Biol 2013, 1040:85–90
31. Aachoui Y, Sagulenko V, Miao EA, Stacey KJ: Inflammasome-mediated pyroptotic and apoptotic cell death, and defense against infection. Curr Opin Microbiol 2013, 16:319–326
32. Rathinam VA, Vanaja SK, Fitzgerald KA: Regulation of inflammasome signaling. Nat Immunol 2012, 13:333–342
33. Yap GS, Ling Y, Zhao Y: Autophagic elimination of intracellular parasites: convergent induction by IFN-gamma and CD40 ligation? Autophagy 2007, 3:163–165
34. Saitoh T, Fujita N, Jang MH, Uematsu S, Yang BG, Satoh T, Omori H, Noda T, Yamamoto N, Komatsu M, Tanaka K, Kawai T, Tsujimura T, Takeuchi O, Yoshimori T, Akira S: Loss of the autophagy protein Atg16L1 enhances endotoxin-induced IL-1beta production. Nature 2008, 456:264–268
35. Zhou R, Yazdi AS, Menu P, Tschopp J: A role for mitochondria in NLRP3 inflammasome activation [Erratum appeared in Nature 2011, 475:122]. Nature 2011, 469:221–225
36. Rathinam VA, Vanaja SK, Waggoner L, Sokolovska A, Becker C, Stuart LM, Leong JM, Fitzgerald KA: TRIF licenses caspase-11-dependent NLRP3 inflammasome activation by Gram-negative bacteria. Cell 2012, 150:606–619
37. Lutz MB, Kukutsch N, Ogilvie AL, Rössner S, Koch F, Romani N, Schuler G: An advanced culture method for generating large quantities of highly pure dendritic cells from mouse bone marrow. J Immunol Methods 1999, 223:77–92
38. Rayamajhi M, Humann J, Penheiter K, Andreasen K, Lenz LL: Induction of IFN-alphabeta enables Listeria monocytogenes to suppress macrophage activation by IFN-gamma. J Exp Med 2010, 207: 327–337
39. Gurung P, Malireddi RK, Anand PK, Demon D, Vande Walle L, Liu Z, Vogel P, Lamkanfi M, Kanneganti TD: Toll or interleukin-1 receptor (TIR) domain-containing adaptor inducing interferon-beta (TRIF)-mediated caspase-11 protease production integrates Toll-like receptor 4 (TLR4) protein- and Nlrp3 inflammasome-mediated host defense against enteropathogens. J Biol Chem 2012, 287:34474–34483
40. Ivashkiv LB, Donlin LT: Regulation of type I interferon responses. Nat Rev Immunol 2013, 14:36–49
41. Rikihisa Y: Ehrlichia subversion of host innate responses. Curr Opin Microbiol 2006, 9:95–101
42. Trinchieri G: Type I interferon: friend or foe? J Exp Med 2010, 207: 2053–2063
43. Zhang Y, Thai V, McCabe A, Jones M, MacNamara KC: Type I interferons promote severe disease in a mouse model of lethal ehrlichiosis. Infect Immun 2014, 82:1698–1709
44. Kuida K, Lippke JA, Ku G, Harding MW, Livingston DJ, Su MS, Flavell RA: Altered cytokine export and apoptosis in mice deficient in interleukin-1 beta converting enzyme. Science 1995, 267:2000–2003
45. Ismail N, Olano JP, Feng HM, Walker DH: Current status of immune mechanisms of killing of intracellular microorganisms. FEMS Microbiol Lett 2002, 207:111–120
46. Ismail N, Walker DH: Balancing protective immunity and immunopathology: a unifying model of monocytotropic ehrlichiosis. Ann N Y Acad Sci 2005, 1063:383–394
47. Meunier E, Dick MS, Dreier RF, Schurmann N, Broz DK, Warming S, Roose-Girma M, Bumann D, Kayagaki N, Takeda K, Yamamoto M, Broz P: Caspase-11 activation requires lysis of

pathogen-containing vacuoles by IFN-induced GTPases. Nature 2014, 509:366–370
48. Hameg A, Apostolou I, Leite-De-Moraes M, Gombert JM, Garcia C, Koezuka Y, Bach JF, Herbelin A: A subset of NKT cells that lacks the NK1.1 marker, expresses CD1d molecules, and autopresents the alpha-galactosylceramide antigen. J Immunol 2000, 165:4917–4926
49. Yang Y, Ueno A, Bao M, Wang Z, Im JS, Porcelli S, Yoon JW: Control of NKT cell differentiation by tissue-specific microenvironments. J Immunol 2003, 171:5913–5920
50. Fang R, Ismail N, Soong L, Popov VL, Whitworth T, Bouyer DH, Walker DH: Differential interaction of dendritic cells with Rickettsia conorii: impact on host susceptibility to murine spotted fever rickettsiosis. Infect Immun 2007, 75:3112–3123
51. Thirumalapura NR, Stevenson HL, Walker DH, Ismail N: Protective heterologous immunity against fatal ehrlichiosis and lack of protection following homologous challenge. Infect Immun 2008, 76: 1920–1930
52. Tekkesin N, Taga Y, Sav A, Almaata I, Ibrisim D: Induction of HGF and VEGF in hepatic regeneration after hepatotoxin-induced cirrhosis in mice. Hepatogastroenterology 2011, 58:971–979
53. Thirumalapura NR, Crossley EC, Walker DH, Ismail N: Persistent infection contributes to heterologous protective immunity against fatal ehrlichiosis. Infect Immun 2009, 77:5682–5689
54. Casson CN, Copenhaver AM, Zwack EE, Nguyen HT, Strowig T, Javdan B, Bradley WP, Fung TC, Flavell RA, Brodsky IE, Shin S: Caspase-11 activation in response to bacterial secretion systems that access the host cytosol. PLoS Pathog 2013, 9:e1003400
55. Broz P, Ruby T, Belhocine K, Bouley DM, Kayagaki N, Dixit VM, Monack DM: Caspase-11 increases susceptibility to Salmonella infection in the absence of caspase-1. Nature 2012, 490:288–291
56. Aachoui Y, Leaf IA, Hagar JA, Fontana MF, Campos CG, Zak DE, Tan MH, Cotter PA, Vance RE, Aderem A, Miao EA: Caspase-11 protects against bacteria that escape the vacuole. Science 2013, 339: 975–978
57. White E: Autophagic cell death unraveled: pharmacological inhibition of apoptosis and autophagy enables necrosis. Autophagy 2008, 4: 399–401
58. Niu H, Xiong Q, Yamamoto A, Hayashi-Nishino M, Rikihisa Y: Autophagosomes induced by a bacterial beclin 1 binding protein facilitate obligatory intracellular infection. Proc Natl Acad Sci USA 2012, 109:20800–20807
59. Leventhal JS, He JC, Ross MJ: Autophagy and immune response in kidneys. Semin Nephrol 2014, 34:53–61
60. Levine B, Kroemer G: Autophagy in the pathogenesis of disease. Cell 2008, 132:27–42
61. Fang L, Li X, Luo Y, He W, Dai C, Yang J: Autophagy inhibition induces podocyte apoptosis by activating the pro-apoptotic pathway of endoplasmic reticulum stress. Exp Cell Res 2014, 322:290–301
62. Yuan K, Huang C, Fox J, Laturnus D, Carlson E, Zhang B, Yin Q, Gao H, Wu M: Autophagy plays an essential role in the clearance of Pseudomonas aeruginosa by alveolar macrophages. J Cell Sci 2012, 125:507–515
63. Nakahira K, Haspel JA, Rathinam VA, Lee SJ, Dolinay T, Lam HC, Englert JA, Rabinovitch M, Cernadas M, Kim HP, Fitzgerald KA, Ryter SW, Choi AM: Autophagy proteins regulate innate immune responses by inhibiting the release of mitochondrial DNA mediated by the NALP3 inflammasome. Nat Immunol 2011, 12:222–230
64. Mihalache CC, Simon HU: Autophagy regulation in macrophages and neutrophils. Exp Cell Res 2012, 318:1187–1192
65. Eskelinen EL, Saftig P: Autophagy: a lysosomal degradation pathway with a central role in health and disease. Biochim Biophys Acta 2009, 1793:664–673
66. Matsuzawa T, Fujiwara E, Washi Y: Autophagy activation by interferon-gamma via the p38 mitogen-activated protein kinase signalling pathway is involved in macrophage bactericidal activity. Immunology 2014, 141:61–69
67. Karim MR, Kanazawa T, Daigaku Y, Fujimura S, Miotto G, Kadowaki M: Cytosolic LC3 ratio as a sensitive index of macroautophagy in isolated rat hepatocytes and H4-II-E cells. Autophagy 2007, 3:553–560
68. Li H, Wang P, Yu J, Zhang L: Cleaving beclin 1 to suppress autophagy in chemotherapy-induced apoptosis. Autophagy 2011, 7: 1239–1241
69. Sun Q, Gao W, Loughran P, Shapiro R, Fan J, Billiar TR, Scott MJ: Caspase 1 activation is protective against hepatocyte cell death by up-regulating beclin 1 protein and mitochondrial autophagy in the setting of redox stress. J Biol Chem 2013, 288:15947–15958
70. Mansueto P, Vitale G, Cascio A, Seidita A, Pepe I, Carroccio A, di Rosa S, Rini GB, Cillari E, Walker DH: New insight into immunity and immunopathology of Rickettsial diseases. Clin Dev Immunol 2012, 2012:967852
71. Pilla DM, Hagar JA, Haldar AK, Mason AK, Degrandi D, Pfeffer K, Ernst RK, Yamamoto M, Miao EA, Coers J: Guanylate binding proteins promote caspase-11-dependent pyroptosis in response to cytoplasmic LPS. Proc Natl Acad Sci USA 2014, 111:6046–6051
72. Hagar JA, Miao EA: Detection of cytosolic bacteria by inflammatory caspases. Curr Opin Microbiol 2014, 17:61–66
73. Man SM, Tourlomousis P, Hopkins L, Monie TP, Fitzgerald KA, Bryant CE: Salmonella infection induces recruitment of caspase-8 to the inflammasome to modulate IL-1beta production. J Immunol 2013, 191:5239–5246